The RADAN Series of Compact Pulsed Power Generators and Their Applications

GENNADY A. MESYATS, SERGEI D. KOROVIN, VLADISLAV V. ROSTOV, VALERY G. SHPAK, AND MICHAEL I. YALANDIN

Invited Paper

This paper presents results of development of a compact pulsed power high-voltage generators and high-current electron accelerators of the RADAN series. The basic high-voltage units of RADAN instruments are built around coaxial pulsed forming lines and efficient charging device represented by a Tesla transformer. The fields of applications in science and in practice are rather wide and include formation of nanosecond and subnanosecond voltage and ultrawideband RF pulses, high-power microwave generation, X-ray radiography, radiation physics, chemistry, and biology. The designed technique provided achievements of outstanding specific parameters of dense e-beams, microwaves, and ultrawideband pulses.

Keywords*—*Backward wave oscillator (BWO), electron beam, energy compression, power conversion, pulsed forming line, spark gap, subnanosecond, superradiation, transit time, traveling wave.

I. INTRODUCTION

A great number of powerful stationary high-voltage pulse generators and high-current accelerators [1], [2] providing fundamental research results were developed from the 1960s through the 1980s. However, the need for compact specialized and multifunctional electrophysical instruments was increasing. The retrospective review of studies shows that small-size devices with the energy output of a few joules and electron beam energy of up to 200–300 keV indeed proved to be efficient in the laboratory practice. This equipment was in great demand in pulsed radiography, high-power microwave (HPM) generation, radiation chemistry, physics, and biology. Each field of application had its specific requirements, but a special significance was attached to general properties of devices, including reliability, self-sufficiency, adjustment of output parameters, accuracy of synchronization, and electromagnetic compatibility with other experimental equipment. All these features were taken into account in the development of compact pulse generators of the RADAN family. They served as the basis of various electrophysical instruments and have been used to solve research problems for two decades now. The most interesting results occur with the generation of strong electron beams and electromagnetic radiation (X-ray, optical, and microwave) pulses (Fig. 1).

II. SMALL-SIZE PULSE GENERATORS

A. High-Voltage Nanosecond Pulse Shapers

A high-voltage generator is the heart of a high-power electrophysical pulse instrument. From the practical viewpoint, it is important that it operates at a repetition frequency, has stable parameters, and is compact, self-sufficient, and technologically reproducible. In addition, X-ray testing and power microwave electronics impose specific requirements on the pulse shape, the permissible electromagnetic noise, tightness of units, etc. Even the first models of compact nanosecond generator of types RADAN-150 (150 kV, 2 ns) and RADAN-220 (200 kV, 3 ns) [3] were distinguished for high efficiency and served as part of X-ray apparatuses and electron accelerators [4] (Fig. 2). Those first developments employed commercial pulse capacitors and high- and low-voltage switches (gas spark gaps and thyratrons). Their operational experience revealed some limitations and drawbacks. Therefore, basic units were developed again for the new generation of RADAN pulsers. This resulted in the appearance of improved models of RADAN-303 and RADAN-EXPERT generators (Fig. 3) [5], [6].

The circuitry of all RADAN generators includes a high-voltage pulsed forming line (PFL) with oil insulation, which is charged from a Tesla transformer (TT), a gas spark

Manuscript received September 4, 2003; revised February 8, 2004.
G. A. Mesyats, V. G. Shpak, and M. I. Yalandin are with the Institute of Electrophysics, Ural Division, Russian Academy of Sciences, Ekaterinburg 620016, Russia (e-mail: mesyats@pran.ru; shpak@iep.uran.ru; yalandin@iep.uran.ru).
S. D. Korovin and V. V. Rostov are with the Institute of High Current Electronics, Siberian Division, Russian Academy of Sciences, Tomsk 634055, Russia (e-mail: contact@hcei.tsc.ru; rostov@hcei.tsc.ru).
Digital Object Identifier 10.1109/JPROC.2004.829005

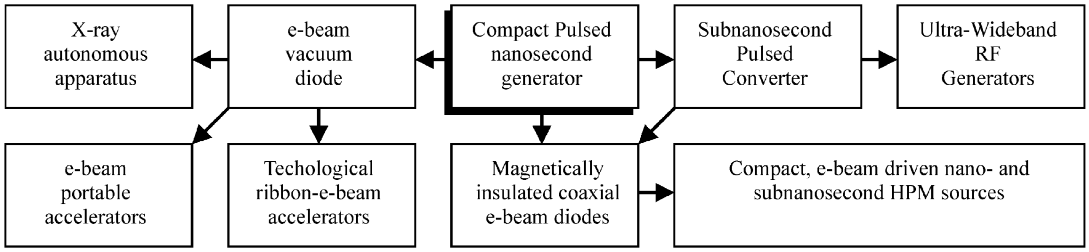

Fig. 1. Fields of application of small-size nanosecond and subnanosecond generators of the RADAN type.

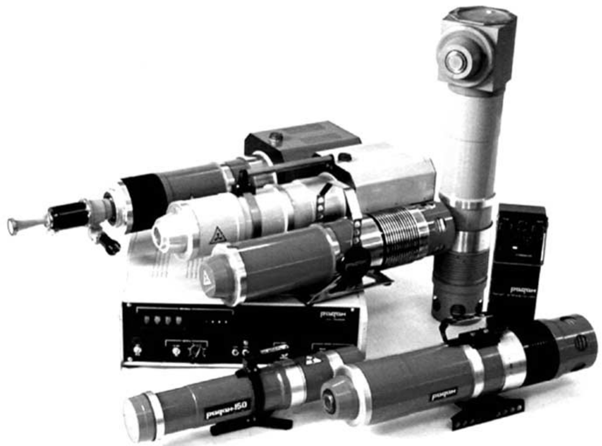

Fig. 2. Nanosecond X-ray apparatus and electron accelerators based on RADAN-150 and RADAN-220 generators.

gap switch, a primary charging device, and monitoring and control systems. The TT coupling coefficient is $\sim(0.7\text{–}0.8)$, which is provided by using of an open steel core. Its magnetic circuits are combined with conductors of the coaxial PFL. The primary and secondary windings of TT are placed in the PFL gap [7]. The open magnetic core ensures the electric strength of the construction and allows placing the whole TT in a screening metal casing. When the PFL discharges, a quasi-rectangular pulse is generated at the load (Fig. 4). The PFL energy capacity is as high as 1 $\mathrm{J/dm^3}$ at the maximum charging voltage of 250 kV, and pulse power in the matched mode is 1 GW. These parameters are limited by the requirement of a reliable operation of the instrument at a pulse-repetition rate of up to 100 Hz, including no-load and short-circuit regimes [8].

When commercial two-electrode high-pressure ($\sim$ 40 atm) hydrogen (P-43) or nitrogen (P-49) spark gaps are used, the PFL charging time (1–1.5 μs) is limited by the electric strength of their ceramic insulators. Fig. 5 illustrates the operational stability of the P-49 spark gap. The maximum of the switching instability of the P-49 spark gap may be due to an irregular illumination of the gap with the spark of an incomplete discharge across the insulator surface [4]. Also, the breakdown mechanism can change with growing pressure owing to initiation of explosive emission at the cathode electrode as soon as the electric field intensity becomes 300–500 kV/cm [9]. The statistical character of these threshold processes leads to a double-humped time distribution of the breakdown dispersion at a pressure of $\sim$ 40 atm

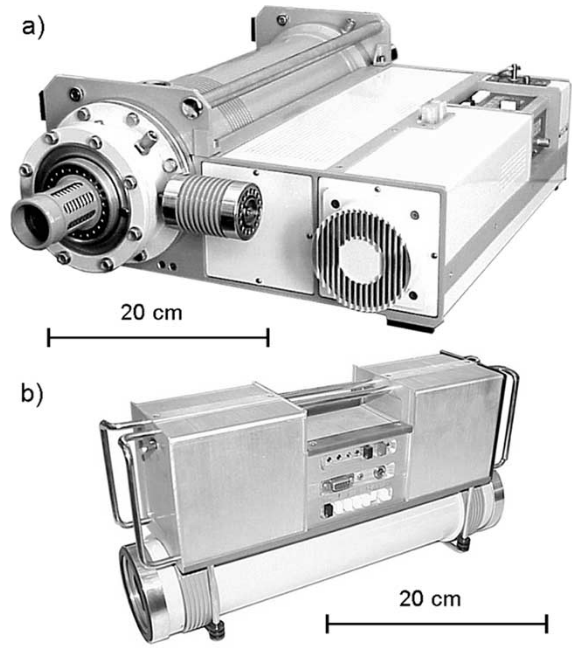

Fig. 3. Nanosecond generators. (a) RADAN-303BP. (b) RADAN-EXPERT.

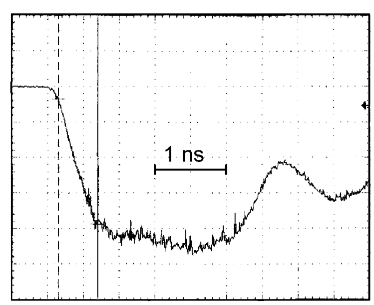

Fig. 4. A 100-kV pulse produced by the RADAN-EXPERT generator.

[Fig. 5(b)]. The dispersion decreases to $\pm$(10–15) ns at lower or higher pressures.

A spark gap, in which one of the electrodes was grounded, was developed for RADAN-303 generators having a pulsed double forming line (PDFL) (Fig. 6). This design provided a simplified adjustment of the gap in the working regime of the generator. If necessary, the working gas could be pumped differently (axially or radially) in the gap. The input of the triggering pulse was simple in the controlled variant of the gas gap switch. The switch commutated at energy of 4–5 J in

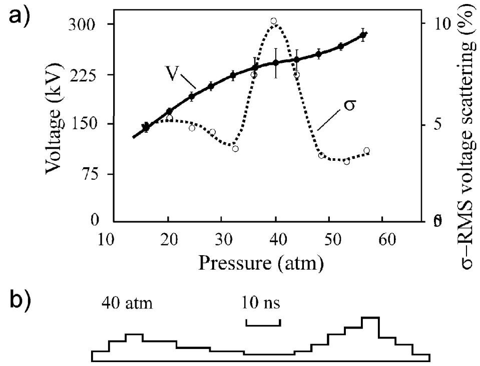

Fig. 5. (a) Breakdown dispersion of a two-electrode gas spark gap depending on the nitrogen pressure. (b) Histogram showing the time variation of triggering of the same spark gap when the PFL is charged at $\sim$ 1.5 μs.

the single regime and up to 2–2.5 J per pulse at the repetition rate of 50–100 Hz. The self-breakdown voltage stability of $\sim$100–200 ns was typical of uncontrolled spark gap with the prebreakdown $dV/dt \sim 10^{10}$ V/s. It was shown that special electrode materials did not outperform copper [10]. Sputtering of the electrodes required that the insulator was cleaned every (1–2) $\times 10^6$ shots.

Technical and service characteristics of a nanosecond pulse-periodic generator largely depend on the circuit design of the primary circuit of the TT, charging devices, and control systems. The TT transformation ratio (100–500) was chosen so as to use standard switches of the primary capacitive storage, which were rated at 3–5 kV (thyratrons, spark gaps), or reduce the charging voltage to the rectified mains voltage if fast thyristors were used. Supply sources of the primary capacitive storage were high-frequency dc-dc converters (the supply voltage of 220 V ac or 12 V dc) or pulsed *C–L–C* circuits having the efficiency of $\sim$0.8–0.9. As a rule, they were designed as a unified module with the PFL and the nanosecond switch (see Fig. 3). The same module hosted control systems [5], [6], which were stable despite the adjacency of the nanosecond generator producing a strong electromagnetic interference. RADAN-303 instruments may be outfitted with redundant control systems having a remote IR communication channel. This is important for experiments with accompanying bremmstrahlung or strong microwave radiation.

As far as the energy efficiency of a nanosecond pulse generator is concerned, charging and commutating devices cause major losses. Ohmic losses in the TT secondary winding prevail in the high-voltage circuit, while commutator losses dominate when the charging time equals units of microseconds. The total efficiency of PFL charging is usually 0.5–0.6. The energy capacity of the PFL at the moment of switching through an uncontrolled gas spark gap generally does not exceed 60%–70% of the maximum value, because the triggering voltage has to be chosen at a level of $\sim$0.8 of the maximum charging voltage. Therefore, misoperations of the gas switch are excluded. Consequently, the “socket-to-load” efficiency of the generator is at a level of 30%–40%. The RADAN nanosecond generators (Table 1) represent electric machines having the overall power of $\sim$10 W/kg at the pulse-repetition rate of 100 Hz. Ohmic losses are distributed over the circuit of the nanosecond generator relatively evenly, without causing local thermal loads.

B. Subnanosecond Pulsed Periodic Generators

Subnanosecond high-voltage pulses are produced by peaking or compression of the energy of nanosecond pulses. The latter method is more efficient from the energy viewpoint. The first subnanosecond high-voltage generators, which were developed on the basis of RADAN nanosecond drivers [11], shortened the pulse by means of high-pressure peaking and chopping gas spark gaps [12]. This converter was called *SLICER*. An improved model compressed the energy by means of an inductive–capacitive compression unit operating under the traveling-wave regime [13]. Both types of the converters allowed adjusting the amplitude, duration, and shape of the pulse. They operated at the pulse-repetition rate of up to 100 Hz (nitrogen) and over 1000 Hz (hydrogen), depending on the gas type [14]. The subnanosecond generators can be used to produce short electron beams [15] or form ultrawideband (UWB) radio frequency (RF) pulses [16], etc.

A broadbandness of the ducts is a mandatory condition imposed on the system of formation and transfer of subnanosecond pulses. The upper bound on the radial dimensions (the slicer represents a coaxial line) is due to the possible excitation of higher waves, which have frequency dispersion. The decrease in the cross-sectional area contradicts the requirement of the electric strength of a high-voltage system. However, the diameter of a 50-Ω coaxial line of the slicer could be reduced to 40 mm for parameters of the peaking pulse of the RADAN-303 generator ($\sim$5 ns, 150–200 kV). With that, the leading edge of $\sim$50 ps can be transferred without distortions. Widening of the leading edge of a pulse decreases due to a special configuration of the spark gap electrodes, which has minimal effect on the interelectrode capacitance and the wave resistance of the coaxial section when the gap is changed [8], [14].

Due to the converter design (Fig. 7), the gas spark gaps can be adjusted within 10 μm in the working regime (at a repetition rate over 100 Hz) without disassembly and depressurization. It is possible to: 1) change the amplitude and duration of the output pulse, while dV/dt of the leading edge remains unchanged (the peaker is fixed and the trailing edge is adjusted); 2) change the leading edge without affecting the amplitude (the trailing edge is fixed and the peaker is adjusted); and 3) alter the three parameters while adjusting both gas spark gaps. Notice that if an inductive–capacitive compression unit is used [13], the amplitude of peaked and shortened pulses is 1.3–1.5 times larger than the amplitude of the initial pulse (Fig. 8). That is, the generator power increases up to $\sim$2 times.

The slicer with a one-gap nitrogen peaking spark gap provided pulses having the amplitude of 100–200 kV and

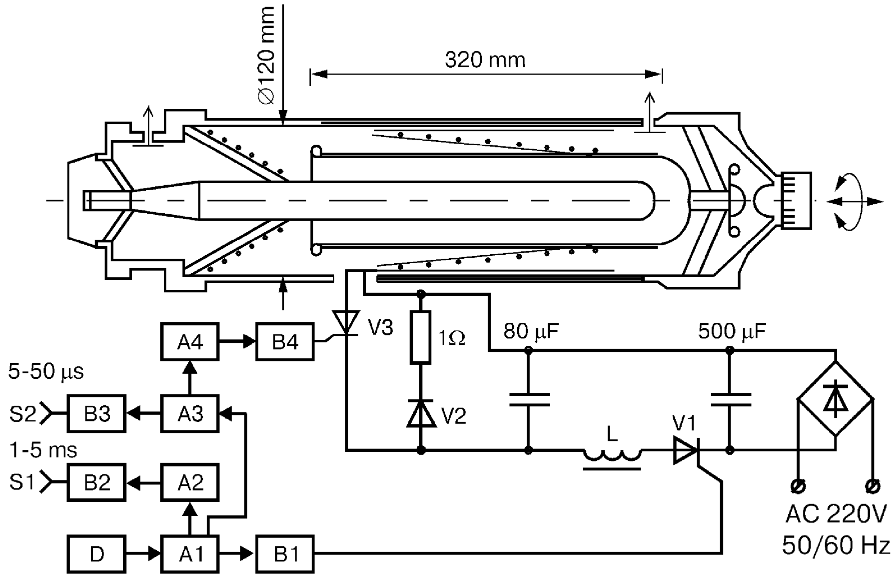

Fig. 6. Design of the high-voltage unit, the spark gap, and the low-voltage circuit of the RADAN-303B PDFL generator.

Table 1
Basic Parameters of High-Voltage Units of RADAN Generators

	RADAN -150	RADAN -220	RADAN -303
Type of the forming line	Single	Single	Double
Impedance, Ohm	22	22	45
Pulse width, ns	2	2	4
Maximum charging voltage, kV	170	220	250
Stored energy, J	0.7	1.2	5
Diameter of the coaxial line, mm	70	102	124
Type of the high-voltage gas switch	P-43	P-49	Special
Primary voltage, kV	3	3 or 5	0.55
Maximum pulse repetition rate, Hz	17	10	100
Maximum power consumption, W	80	100	1000

full-width at half-maximum equal to ~200–500 ps. The leading edge was 150–200 ps when the prebreakdown dV/dt at the peaking gap was $\sim 2 \times 10^{14}$ V/s. As distinct from the peaking gas switch, the chopping spark gap operates under "traveling wave" conditions and at larger dV/dt. Therefore, its gap is much narrower than the peaker gap. Consequently, the commutator spark has lower inductance; hence, the trailing edge is much shorter than the leading edge.

A digital stroboscopic oscilloscope could be used for measurements due to a stable operation of the generators in the pulse periodic regime. The analysis of oscillograms recorded by a Tektronix TDS-820 oscilloscope showed that the amplitude stability of a 250-ps pulse [Fig. 9(a)] was within ± (2–3)% and that of a pulsewidth was within ± 25 ps in the case of peaking and chopping spark gaps filled with nitrogen. If the gap in the chopping spark gap increased (i.e., the pulsewidth increased, specifically, to 500 ps), the instability of the breakdown was ± (50–100) ps [Fig. 9(b)]. The reason was the decrease in the overvoltage. Note that at the prebreakdown $dV/dt \sim 0.2 \times 10^{15}$ V/s, the time instability of the peaker triggering was about 100 ps. This was demonstrated using a two-channel nanosecond generator with independent peaking spark gaps [17].

Characteristics of the formed pulses remained generally unchanged when the spark gaps were filled with hydrogen up to a pressure of 100 atm. However, since hydrogen quickly recovered its electric strength after a breakdown, it was possible to operate at a repetition rate of up to 3500 Hz without gas circulation. The breakdown voltage of the peaking hydrogen spark gap did not decrease at the commutation energy of ~1 J. A repetition rate of up to 3500 Hz was achieved thanks to the use of a nanosecond modulator with a solid-state commutation system based on semiconductor opening switch (SOS) current interrupters [18].

C. Synchronization of High-Voltage Generator

Compact nanosecond generators and high-current accelerators are used on a wider scale in physical experiments if they are made more stable and are synchronized very accurately. These opportunities are realized by several methods. The microsecond synchronization of a generator is provided by means of controlled commutators in the low-voltage circuit of TT: spark gaps, thyratrons, or thyristors. The triggering accuracy of the last two types of switches is much better than 1 μs, while the total dispersion of the triggering time depends on characteristics of the high-voltage spark gap (see Fig. 5) [4]. The RADAN-220 generator with a two-electrode high-voltage spark gap [19] was synchronized to within ± 1 ns using a laser pulse. Later on, laser methods of synchronization were rejected because of the complexity of laser systems.

An alternative method for precision triggering of a high-voltage spark gap is the electric pulse control. As noted, the feed of a subnanosecond triggering pulsewith $dV/dt \sim 10^{15}$ V/s to the discharge gap does not present

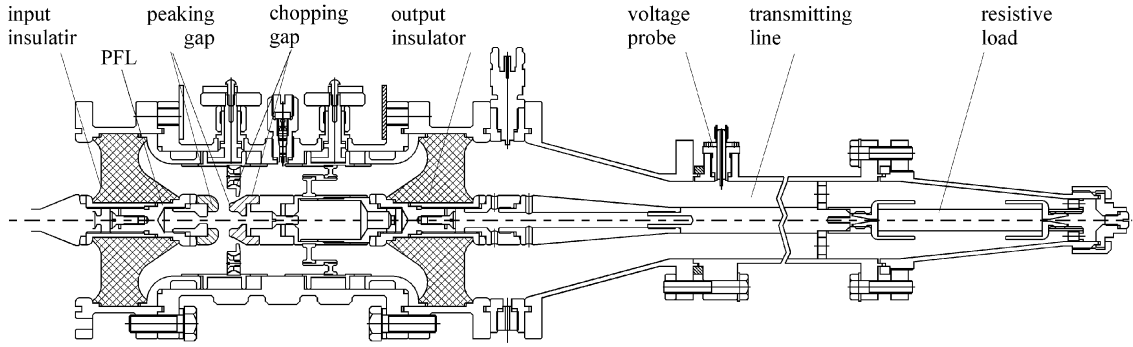

Fig. 7. Design of a subnanosecond converter with peaking and chopping spark gaps.

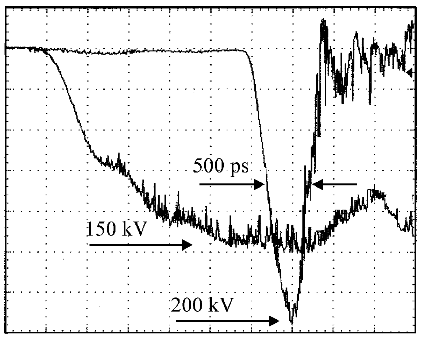

Fig. 8. A 150-kV pulse of a nanosecond generator and the pulse transformed in the inductive–capacitive compression unit after additional shortening by the chopping spark gap.

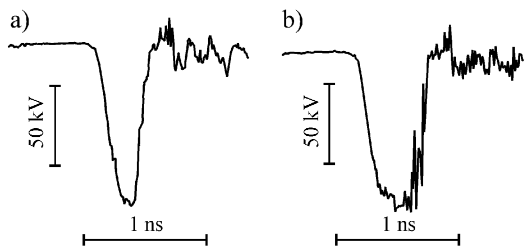

Fig. 9. Pulses formed by a subnanosecond slicer at different switching delays of the chopping spark gap.

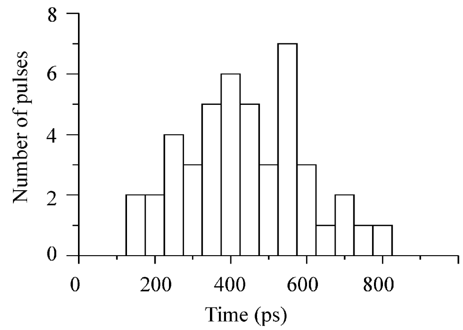

Fig. 10. Histogram of synchronization of pulses from a two-channel subnanosecond generator equipped with controlled nanosecond spark gaps.

any problem in PDFL generators of the RADAN-303 type, in which one electrode of the switch is grounded. A subnanosecond accuracy of the spark gap triggering at a minimal amplitude and the shortest triggering pulse is important from the practical viewpoint. These conditions are provided when a subnanosecond controlling pulse produces high electric field at the negative triggering electrode, which is comparable with the field in spark gap of a subnanosecond slicer [8], and a leading subnanosecond breakdown is ensured between the triggering electrode and the opposite potential electrode. Computer simulation and subsequent experiments [20] demonstrated the possibility to achieve required overvoltages at the control pulse amplitude of 15–50 kV. If the triggering pulse is generated by a subnanosecond converter [8], it allows splitting to supply of up to ten spark gaps for synchronous triggering. Since the pulsewidth does not exceed 0.3 ns, it is this value that can be assumed as the upper estimate of the achieved accuracy of the spark gap triggering. It was shown that when a spark gap is triggered at a voltage 5%–7% smaller than the self-breakdown voltage, the ratio between the energy of the control pulse and the energy stored in the PDFL does not exceed 10^{-3}.

An experiment concerned with synchronization of two subnanosecond generators using controlled high-voltage spark gaps was performed [17]. The experimental setup included three nanosecond PDFL switches and eight subnanosecond discharge gaps. The data on the relative variation of subnanosecond edges of the formed pulses (Fig. 10) showed that it was possible to synchronize high-power multichannel generators with the pulse length of 0.5–1 ns.

The information about the triggering accuracy of controlled high-voltage spark gaps is important for improvement of the amplitude stability of output pulses of a nanosecond generator. The stability $\Delta V/V = (dV/dt)\Delta t < 10^{-3}$ can be achieved at microsecond charging of the PDFL and the subnanosecond triggering accuracy. The stability is limited in practice by the triggering time variation of the triggering pulse generator. For example, the amplitude variation was $< 10^{-2}$ at 8-μs charging of the PDFL and 50-ns time spread of the triggering pulse [21].

By design, the high-voltage spark gap, in which one of the electrodes is grounded, provides an option of simultaneous triggering of several PDFL generators by means of a combined switch [17]. A specific feature of this method is the parallel connection of PDFLs during charging. They discharge independently to a separate load each. In this case, nanosecond pulses have equal amplitudes and are free of mutual jitter.

III. Generators of Ultrawideband Radio Frequency Pulses

Pulse generators transfer the energy to a load as a transverse electromagnetic (TEM) wave. It can be converted to a UWB electromagnetic pulse during radiation from a TEM antenna. This radiation of the RF band presents interest for radiolocation, reliability tests of electronic equipment, etc. [22]. Reproducibility of spectral characteristics of UWB RF pulses fully depends on stability of the feeding generator.

In the simplest case, a stepwise voltage differential of the required steepness may be applied to the antenna. However, the long-time effect of the voltage requires an increased electric strength of the feeder between the generator and the antenna. Therefore, the most compact versions are powerful UWB generators supplied by short "rise–fall" voltage pulses. These requirements are satisfied by subnanosecond shapers based on RADAN generators providing pulses of hundreds of megawatts [8], [11]. The shape of the pulse for excitation of the TEM antenna is chosen considering its matching with the modulator and an efficient conversion of the energy to radiation. Bipolar pulses are preferable in this respect. Their spectral function turns to zero in the limit of lower frequencies. A subnanosecond unipolar pulse of the slicer is transformed to a bipolar pulse using an adjustable closed stub [23]. Bipolar pulses ($\sim 2 \times 500$ ps) with a double amplitude differential (± 140 kV) are formed in a device including a short capacitive storage and two uncontrolled gas spark gaps operated with a relative scatter of ± 100 ps [11].

A drawback of UWB radiators is the difficulty of shaping a low-divergence radiation pattern. A high-power one-channel radiator is an alternative to narrow-pattern pulse antenna arrays with synchronized low-power elements. Let it be noted, however, that subnanosecond generators of the RADAN type with precision synchronization or a combined switch can be used for creation of UWB antenna arrays and those with high-power channels. Fig. 11(a) presents a typical directional pattern of a high-voltage TEM antenna with aperture 30×30 cm in size [16] supplied by a unipolar feed pulse 300 ps long and 100 kV in amplitude. The maximum radiation electric field at a distance of 25 m was 140 V/cm. The directional pattern peaks [Fig. 11(b)] if a split pulse is fed to the TEM antenna array [23]. If several TEM horns are connected to synchronized pulse generators, the UWB RF pulse gains in power in the main direction of the antenna system (Fig. 12).

In experiments with UWB radiators based on RADAN generators, matching junctions and TEM antennas were in air at atmospheric pressure. The external diameter of 50-Ω feeders of the antenna was 36–70 mm. Since the length and the amplitude of pulses could be adjusted, it was possible to obtain information about the electric strength of the insulation in the subnanosecond range [24]. Specifically, the electric strength of air for unipolar signals (250 ps, -100 kV) was five times larger than the static strength (Fig. 13). The measurements were made at a pulse-repetition rate of 100 Hz when the antenna received a signal having the peak power of 200 MW.

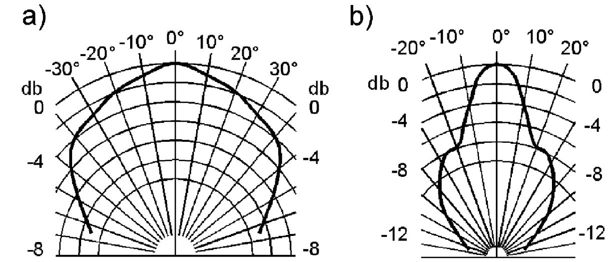

Fig. 11. (a) Directional pattern of a high-voltage TEM horn with a 30×30 cm aperture. (b) Two-dimensional antenna array of four TEM horns with the space base of 1.35 m in the H plane.

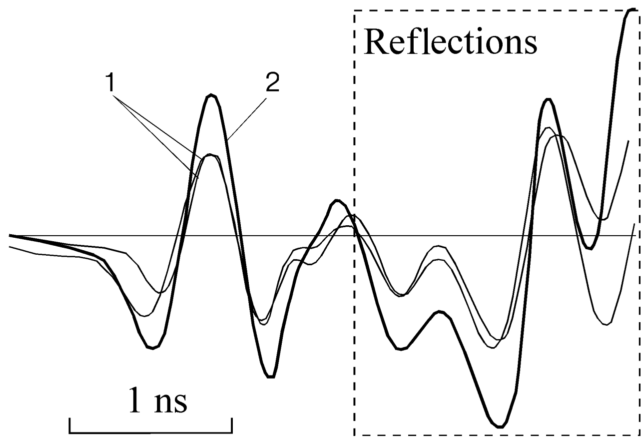

Fig. 12. Recording of UWB signals using a pilot discone antenna at a distance of ~ 20 m in the main direction from a two-channel generator. 1—Operation of separate modules. 2—Synchronous summation of radiation.

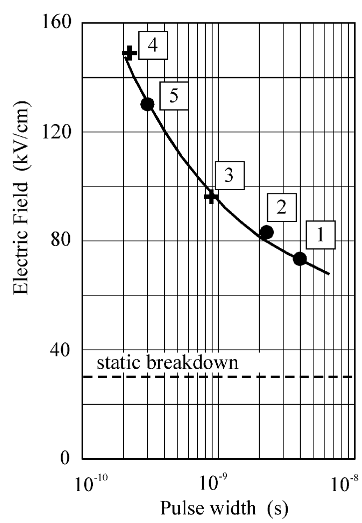

Fig. 13. Critical electrical field, which corresponds to appearance of a discharge in the atmospheric air, versus the voltage pulsewidth. Effects: 1—37-GHz BWO. 2—35-GHz TWT. 3, 4—unipolar voltage pulses. 5—38-GHz SR pulse.

IV. Sources of Electrons and X-Ray Radiation

A. *Self-Contained X-Ray Apparatuses and Electron Accelerators*

Self-contained X-ray apparatuses, which are based on RADAN-150 and RADAN-220 nanosecond generators [3],

Fig. 14. Roentgenogram of the contents of hand baggage obtained at 5-s exposure. Shooting distance is 0.7 m.

[4], employ commercial uncontrolled gas spark gaps in the primary and secondary circuits of the TT and sealed-off cold-cathode X-ray tubes (IMA type) with explosive emission of electrons. The working voltage of these components is fixed; hence, output parameters of the X-ray units cannot be adjusted. Several units with different tube voltages are required to extend the range of object density available for operative radiography.

The compact portable RADAN-EXPERT apparatuses [6] (Figs. 3 and 6) are equipped with a gas spark gap, which can be adjusted to two fixed breakdown voltages (90 and 150 kV). The adjustment does not require depressurization of the gas switch and is realized by altering the working gap with the help of the movable electrode, which has an inertial drive mechanism. Since the charging device of the high-voltage generator is highly efficient, it can operate from power mains or a 12-V storage battery. One pulse of the RADAN-EXPERT apparatus provides a dose of 0.35×10^{-3} roentgens at a distance of 500 mm. The capacity of the storage battery (4 A $\cdot$ h) is sufficient for producing 10^4 pulses at a repetition rate of 5–10 Hz or ~ 200 five-second exposures (Fig. 14).

RADAN X-ray apparatuses equipped with IMA tubes were used, along with X-ray flaw detection [3], in studies of biological and therapeutic effects of pulsed X-ray radiation. A maximum integral irradiation dose over the whole spectrum was significant for those experiments. It was shown for a single-PFL generator [25] that the mismatched operation of the generator and the load was most favorable in energy terms, when the impedance of the X-ray tube was five to six times larger than the PFL impedance ($\sim 20\ \Omega$).

Pulsed cathode luminescence, radiation-chemical processes, and surface sterilization were studied using sealed-off cold-cathode tubes with beryllium foil windows for injection the electron beam to the atmosphere. The transparency limit of the foil requires that most of the generator energy is concentrated in the main accelerating pulse and reflections are minimized. Otherwise, low-energy electrons are absorbed and heat the foil. If an IMA3–150E sealed-off e-beam diode is used, preference is given to RADAN-303 PDFL generators having an impedance of 50 Ω. They can transmit over

Fig. 15. System of two sealed-off e-beam vacuum diodes of a laboratory technological accelerator, which are placed in a compact protective chamber.

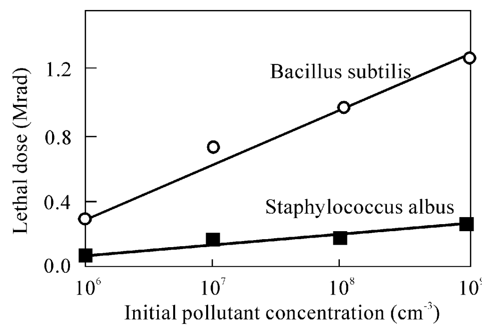

Fig. 16. One hundred percent lethal dose of surface sterilization for some bacteria.

50% of the energy to the main pulse of the electron beam without matching lines. The RADAN-303 generator can operate with several parallelly connected e-beam diodes. Such a system with two diodes and a rotating object stage placed in a compact protective chamber (Fig. 15) served as the basis of a pulsed accelerating installation, which was used for development of radiation technologies, examination of the effect of pulsed beams on microorganisms, etc. [26]. Sliding joints of the feeders make it possible to change the orientation of the diodes, i.e., the electron irradiation zone. In the case of a two-sided treatment at a frequency of 10–15 Hz, the surface sterilization of objects ~ 80 mm in diameter is complete in 10–20 s (Fig. 16). If the service life of the e-beam diodes is $\sim 10^5$ pulses, the number of treatment operations is $\sim 10^3$. A twofold drop of the dose per pulse is taken as the limit of diode service life.

B. Electron Accelerators With Wide-Aperture Beams

The use of sealed-off e-beam diodes makes the operation of accelerators quite easy. However, the work with these systems in technological radiation studies is complicated owing to a limited service life of the cathodes and the foil windows. Continuous-pumping wide-aperture diodes, which allow replacement of the cathode and the foil window, can be used more conveniently in such studies. Extensive (ribbon) diodes are matched with the voltage generator in a specific way. If the pulse length is comparable with the transit time of the diode, it operates in the traveling-wave regime. This design is called the traveling-wave diode (TWD) [27]. The diode represents a generator-matched vacuum coaxial line, whose electric length is longer than the pulse rise time, but does not exceed the pulse length. A high-voltage pulse is applied to the line input. The pulse is reflected at the opposite open end of the line and moves back. The long cathode is switched as the incident wave is passing. The ribbon electron beam, which is formed, serves as the distributed load of the long line with losses. The voltage at each section of the anode–cathode gap is the sum of voltages of the incident and reflected pulses. Therefore, the set of parameters (the electron energy, the beam current, and the pulse length) differs considerably at each point of TWD. A uniform integral energy yield of the beam along the diode is possible if the anode–cathode gap is nonuniform (increases) on the diode length. In this case, a low voltage at the TWD input is compensated by a longer operating time of the initial section of the cathode. This was confirmed by calorimetric measurements of the beam energy behind the foil. Diodes 110 and 500 mm long employed a cold cathode whose operation depends on explosion emission at the "metal–dielectric–vacuum" triple point. They had an easy-off foil window 35–50 μm thick made of an Al–Be pseudoalloy (50%–50%), which is distinguished for good thermal conductivity and sufficient electron transparency. The system could operate continuously at repetition rates of up to 25 Hz. The lifetime of the window was at least 10^6 pulses at the current density of 70–300 $\mathrm{A/cm^2}$. Since the foil can be replaced quickly, these parameters are quite sufficient for experiments on radiation-chemical treatment of polymers, surface sterilization, etc.

C. Magnetically Insulated Electron Beams

High-current magnetically insulated electron beams of nano- and subnanosecond duration are widely used in studies concerned with mechanisms of generation of a strong microwave radiation and development of HPM generators with an extensive energy-exchange space [2], [28]. Magnetic isolation is necessary for both the formation of the beam in the accelerating gap and the beam guiding in the drift chamber of the accelerator. When the length of accelerating pulses is 3–5 ns, which is typical of nanosecond pulse generators of the RADAN type, the formation of electron beams in a magnetically insulated vacuum diode encounters the same problems as in systems with pulses 10–100 ns long. They differ in compactness of the short-pulse vacuum diode and a small cross size of the drift chamber of the accelerator. In particular, a permanent magnet (NdFeB) can be used for a vacuum diode with the drift chamber 10 mm in diameter. The magnet produces a quasi-solenoidal magnetic field of

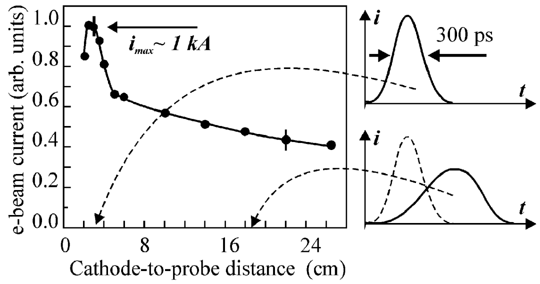

Fig. 17. Current pulse amplitude of a subnanosecond beam depending on the guiding length along the drift chamber of the accelerator.

1.4 T [29]. The problem of reversing the field at edges of the magnetic system is solved by the embodiment, in which the magnet fully encloses the inlet insulator of the vacuum diode and the accelerator cathode 2.5 mm in diameter is located in a homogeneous field.

Capacitor bank-powered pulsed magnetic coils are widely used for focusing of nanosecond and subnanosecond high-current beams. Superconducting magnetic coils and liquid-cooled dc magnetic coils are used too. In the latter case, stabilized power is supplied from a bank included molecular capacitors and a transistor insulated gate bipolar transistor (IGBT) switch operating in the pulsewidth modulation regime [30].

When the accelerating pulse length is less than a nanosecond, the formation of a high-current beam has some specific features arising from the longitudinal dynamics of electrons and a finite initiation time of the cathode emission. These processes, which have the characteristic time scale of about 10^{-10}s, can be recorded using real-time oscilloscopes and special current transducers. For example, the experiments in [15] demonstrated that a nanosecond prepulse is significant for initiation of the cathode emission. As the action time of relatively low-voltage prepulse increases, the cathode injects a larger current even if the length of the accelerating subnanosecond pulse is shorter. Significantly, not only the amplitude of the current pulse, but also the integral charge of the beam increase in this regime.

An irregular shape of a subnanosecond pulse of the accelerating voltage (see Figs. 8 and 9) determines a dynamic behavior of the longitudinal structure of the beam. The space charge of electrons, which are emitted at a maximum accelerating voltage, accelerates additionally the preceding low-energy fraction at the inlet to the drift chamber. Hence, the leading edge of the beam current peaks and the current amplitude reaches a maximum at some distance from the cathode. The increase in the transportation length causes a drop of the current and smearing of the beam duration (Fig. 17). Moreover, some electrons receive a considerable additional acceleration (up to $\sim$1.5–fold by the energy) depending on the drift length. These data were obtained from the analysis of the penetration depth of a beam through packages of dosimetric films [31] and were in qualitative agreement with the dynamics of the beam leading edge, which was analyzed by the time-of-flight method. Notice that the time-of-flight measurements were possible due to a

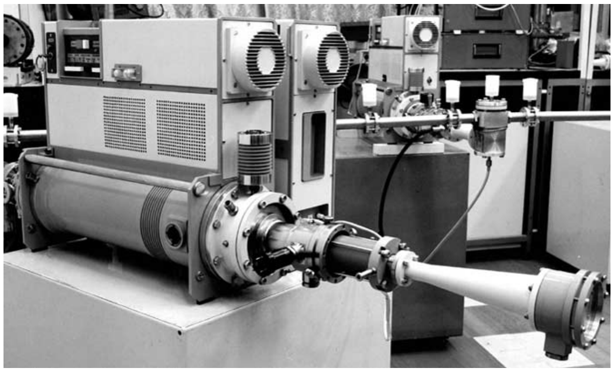

Fig. 18. MG-4R microwave generator rated at 35 GHz employing backward wave tube.

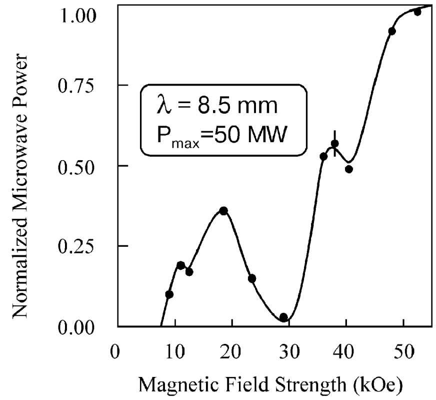

Fig. 19. Thirty-five gigahertz BWO generation power dependence on the guiding magnetic field.

stable operation of the high-current subnanosecond accelerator and the resolution of the recording equipment at a level of 10–20 ps. The additional acceleration mechanism could be self-acceleration of some electrons in the field of a space charge wave, which was excited in a dense electron flow. This supposition was confirmed by a full-scale numerical experiment [32].

The data concerning specific features of generation and dynamics of short rectilinear high-current beams were necessary for development and adjustment of a more complicated system for pumping of transversal velocities of an electron beam in a gyroresonance microwave device [33]. The time-of-flight method was used for direct estimation of such a complicated characteristic as the ratio between the transverse and longitudinal velocities of magnetized electrons at the beam leading edge.

V. Generation and Amplification of High-Power Microwave Radiation

A. Nanosecond Sources of High-Power Millimeter Wavelength Radiation

Since pioneering studies into HPM generation (in the 1970s and 1980s), efforts of researchers at the Institute of Applied Physics, Nizhny Novgorod, Russia, and the Institute of High Current Electronics, Tomsk, Russia, have resulted in a comprehensive theoretical understanding and advanced practical applications of *X*-band relativistic backward wave oscillators (BWO) [34], [35]. An attempt to project the obtained results to the millimeter wavelength band [36] showed that it was necessary not only to miniaturize BWO electrodynamic systems, but also to develop specialized high-current accelerators [2]. The energy of the accelerator was difficult to convert fully to the energy of a microwave pulse in the existing experimental setups. However, new microwave devices found their users (radiobiology, medicine, electronics, etc.) who required small-size, cheap and self-contained HPM sources. It is with this situation in mind that the work was initiated in 1980 aimed at creation of HPM millimeter-wavelength oscillators employing small-size accelerating equipment [37], [38].

New BWOs of the MG type, Ka-band microwave oscillators based on RADAN accelerators (Fig. 18) use weakly relativistic magnetized high-current beams having an energy of 150–200 to 300 keV [39]. In the lower limit of the electron energy, it is difficult to provide optimal conditions of the beam energy exchange with the synchronous space harmonic of the wave TM_{01} excited in a slow-wave system (SWS). Therefore, when a uniform SWS was used, the efficiency of the beam power conversion to the radiation power (the power conversion) in the quasi-stationary oscillation regime was a few percent. The peak power did not exceed 10 MW in the first experiments [37], [38]. The power increased to 40–60 MW when a nonuniform SWS was introduced and the beam energy increased to 280–300 keV. The power conversion factor was as large as 10%–15% at frequencies of 35 and 70 GHz [39].

It is pertinent to mentioned that, for the typical mismatch of (20–50)-Ω voltage generator and high-ohmic e-beam injector (see, e.g., Fig. 4), there is a certain probability of excitation of parasitic microwave generation due to the electron beam generated at low-voltage reflected pulse. This generation, however, can be suppressed by proper choice of beam-to-wave coupling.

SWS breakdown-initiated pulse shortening of microwave generation could be avoided in an HPM device with the beam length of < 5 ns. This limitation was found for quasi-stationary *X*-band generators with the beam length exceeding 10 ns (see, e.g., [40]). It considerably impaired the performance of microwave generators. In our case, the radiation power density in the SWS with the cross section $\sim \lambda^2$ can be increased considerably (by a factor of two to four). The SWS breakdowns are not observed or, at least, do not affect the device performance. Thus, the power density of up to 0.5 GW/cm^2 is achieved in the SWS at the generation duration of 3–4 ns. The electric field strength of the wave on the SWS walls is ~ 1 MV/cm. Microwave generators remain serviceable in a technical vacuum of $\sim 10^{-2}$ torr.

Widening caused by transverse expansion of the cathode plasma in crossed fields of the vacuum diode is insignificant for beams, which are units of nanoseconds long. However, the beam geometry requirements impose strict limitations on the magnitude of the guiding magnetic field. Tubular beams having the diameter of 2–5 mm, the current of ~ 1–2 kA and the current density over 10^4 A/cm^2 should be guided at a distance of ~ 0.2 mm from the SWS wall. Guiding without the loss of current is possible in an axial magnetic field exceeding 20 kOe. An additional limitation is connected with the cyclotron resonance of electrons with the forward propagating wave TM_{01} (in the field of ~ 30 kOe). Consequently, the field of ~ 50 kOe is required so that a maximal power is achieved in 8-mm band BWO [39] (Fig. 19). A pulse magnetic coil working under the rare repetitive duty or a superconducting magnet provides this value.

Some problems arise when the "cyclotron resonance" is approached from the side of small (<20 kOe) fields. The tubular beam is initially ~ 0.5 mm thick. It should be guided at a large distance from the SWS wall; hence, the synchronous wave coupling resistance and the generation efficiency are impaired. Moreover, some fraction of the beam is ejected to the wall as long as electrons acquire large transverse velocities in the field of the generated wave. This process leads to a periodic decrease in the microwave generation power, which resembles automodulation [41]. However, if the magnetic field is small ($\sim$ 15–20 kOe), the power consumption of the pulse magnetic coil changes by one order of magnitude. Such BWOs with the peak power of ~ 20 MW can operate at a repetition rate of up to 10 Hz in the burst mode. No limitations are imposed on the number of pulses in a burst as far as the source of the magnetic field is concerned when the beam in a 70-GHz BWO is focused using a system with high-coercivity permanent magnets NdFeB [29]. In this case, the pulse-repetition rate is limited only by the electron accelerator.

A successful development of MG-type microwave generators allowed studying for the first time the amplification of high-power millimeter wavelength radiation using the Cherenkov mechanism of interaction of high-current beams [38]. The amplifier was a traveling-wave tube with a synchronous forward harmonic of the hybrid wave $TE–TM_{11}$ of a circular corrugated waveguide. A waveguide directional coupler served as the basis of a simple device for feeding of a microwave signal of the magnetron to the interaction space of the amplifier. A short beam eliminated the effect of spurious reflections on the instrument performance. The magnetron signal passed through the SWS toward the electron flow. After the wave was reflected from the cutoff neck, which was located near the "cathodic" side of the SWS, the condition of synchronism between the electrons and the forward space harmonic was fulfilled. The single-mode SWS prevented self-excitation of spurious waves at the working frequency. The amplified microwave signal 2 ns long having megawatt power was fed out through a standard air-filled waveguide without breakdowns. A 100-ns input magnetron signal was sufficient for synchronization with the accelerator beam when the RADAN-220 generator was triggered with an accuracy of ± 15 ns. The region with a pronounced maximum amplification was determined in the adjustment range of the guiding magnetic field and the accelerating voltage. When the coupling coefficient of the beam and the wave was large and the input signal was small (~ 50 W), the gain factor was 30 dB. The gain decreased to 22 dB with growing power of the input wave. The same value of the gain factor (22 dB) was obtained at a smaller coupling coefficient and the input microwave power of ~ 6 kW. In this case, the amplifier worked in the linear regime with an increment of ~ 2 dB/cm and did not show the trend to saturation (Fig. 20). The output power was 1 MW. As distinct from the generator, the amplifier allows the control of output radiation parameters, such as the power level, phase characteristics, etc. Obviously, high-power amplifiers may find an extensive application in practice, specifically, development of devices for coherent summation of power. This task is quite real for systems based on RADAN generators, which provide a subnanosecond accuracy of triggering.

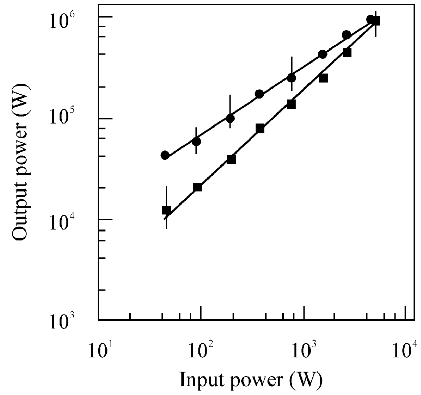

Fig. 20. Gain factor of relativistic Ka-band TWT amplifier realized for two values of coupling between the beam and the wave.

B. Generation of High-Power Subnanosecond Microwave Pulses

Small-size high-current accelerators with the current pulse 0.3–1 ns long were used in studies concerned with nonstationary processes of stimulated microwave radiation of dense relativistic electron beams. From the practical viewpoint, those studies tackled the problem of increasing the conversion of the electron beam power and providing a larger radiation power when effects of shortening of microwave generation, which are related to the breakdown of electrodynamic structures, knowingly have not time to develop. Considered mechanisms for formation of ensembles of classical oscillating electrons, which form a short dense beam, were analogous to the Dicke superradiation (SR) effect known in quantum optics, that is, coherent single-pass amplification of spontaneous radiation [42]. The theory of the cyclotron mechanism of microwave SR of electron flows [43] was confirmed experimentally [33]. Later studies were concerned with SR of instruments based on undulator and Cherenkov microwave radiation (Fig. 21). RADAN accelerators, which were used in those studies, ensured stability and a wide adjustment interval of parameters of electron beams.

In studies of cyclotron SR, a kicker imparted a transverse oscillator velocity to electrons of the beam (300 ps long) at the inlet to the drift chamber. The oscillator velocity was adjusted until pitch factors $g = V_R/V_Z > 1$ were obtained. A fine adjustment of the instrument was possible, since parameters of the electron beam, the kicker fields, and the guiding

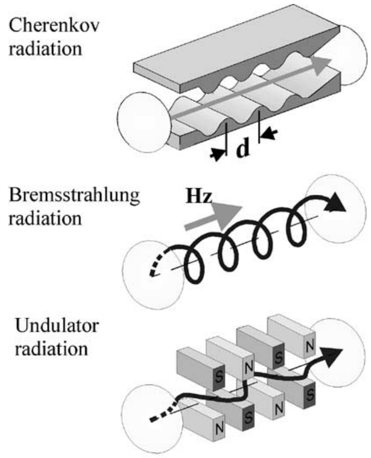

Fig. 21. Schematic circuit diagrams of tested relativistic microwave oscillators having different mechanisms of energy exchange.

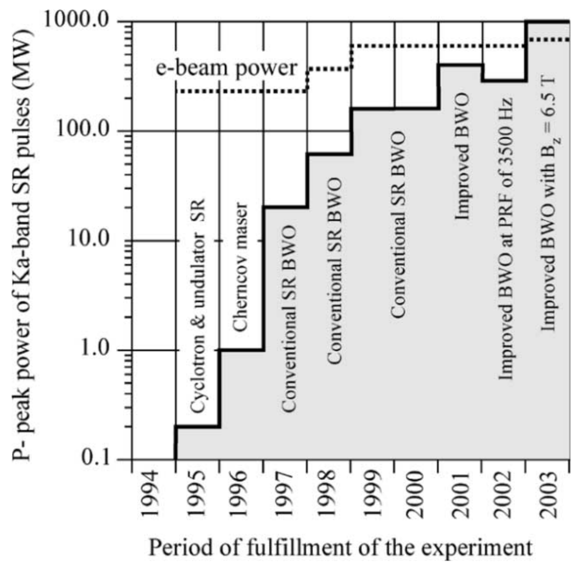

Fig. 22. Results of investigations of superradiative sources in the Ka-band.

magnetic coil could be changed easily. The microwave radiation was a monopulse in the regime of grazing of the dispersion curve. The pulse split if it crossed the dispersion curve. The frequency of the leading edge of the pulse was larger than the frequency of the trailing edge in accordance with the Doppler effect. The radiation power increased exponentially with growing interaction length. This situation is characteristic of the regime of stimulated radiation. The estimated peak power of SR was $\sim$200–400 kW, which corresponded to the transformation of the beam energy equal to $\sim 1\%$. Under conditions of synchronism with the mode TE_{11} of the circular waveguide, SR was also observed when an electron bunch moved in a helical undulator, which was placed in the guiding magnetic field. The maximum peak power of SR equal to hundreds of kilowatts was obtained for a "forward" directed magnetic field, which was as large as 13 kOe [44]. The undulator field was 2 kOe.

Subnanosecond microwave pulses with the leading edge of less than 200 ps and the spectrum integral power of $\sim$1 MW were obtained during interaction of a rectilinear subnanosecond beam (the current of 100–150 A) with synchronous fields of a dielectric SWS. The efficiency of the beam energy transformation in this Cherenkov maser under the SR regime was $\sim 3\%$–5%. The power of the instrument was doubled thanks to the use of a hybrid SWS when a modulating section of the BWO type was installed ahead of a dielectric amplifying structure [45].

The greatest advances in generation of high-power subnanosecond pulses of the millimeter wavelength band were made in experimental studies of SR of high-current electron beams moving in periodic structures of the BWO type (Fig. 22). Theoreticians [46] were the first to note the opportunity to use relativistic BWO for a sharp initial burst of power, which is several times larger than the level of the steady-state generation. This SR regime of generation of millimeter band waves at frequencies of 38, 70, and 140 Hz was realized using RADAN accelerators [47]. Experiments [48] revealed a quadratic dependence of the peak power of SR pulses on the electron beam charge. If a superconducting magnet was used, the SR source operated at a repetition rate of 25–100 Hz.

The conventional schematic of relativistic BWO [34], [39], [40] provided a relatively high peak power of the order of 60–150 MW [47], [48] in the 8-mm wavelength band, but the "beam-radiation" power conversion did not exceed 0.3. Further theoretical studies of the nonstationary regime of relativistic BWO and experiments in the X-band [49] demonstrated that it was possible to obtain short microwave SR pulses with the peak power, which was not limited by the beam power in principle. The essence of this effect was that the energy transfer to a spatially short electromagnetic pulse from relatively extensive beam was realized in a distributed regime, with the counterdirectional movement. Potentialities of compact high-current accelerators were realized to the most extent in this regime providing the power conversion$>$ 1. A BWO with SWS having a large cross section ($S \sim 1.5\lambda^2$) and a bandpass reflector was used in experiments [50]. The space charge of the beam has a less critical effect on the beam bunching in this oscillator. The SWS provides a low dispersion of the wideband wave packet and represents a more convenient channel for the electron transport. This feature is especially important when the axial magnetic field is smaller than that corresponding to the cyclotron resonance. An experimental setup employing a RADAN-303BPM accelerator generated subnanosecond SR pulses 250 ps long with the central frequency of 38 GHz at the guiding magnetic field equal to $\sim$2 T. The pulses had the power of 240–280 MW and the power conversion factor was 50% [51]. These results gave grounds for the next experiment [30], for which a subnanosecond accelerator was made employing a modulator with an all-solid-state switches and a cooled dc solenoid ($B_Z \sim$ 2 T). In this case, 300-MW SR pulses were generated at a repetition rate of 1000–3500 Hz in 1-s bursts [Fig. 23(a)]. The burst-average SR power was $\sim$200 W.

In a recently completed experiment with a RADAN-303BPM accelerator, an optimized electrodynamic BWO

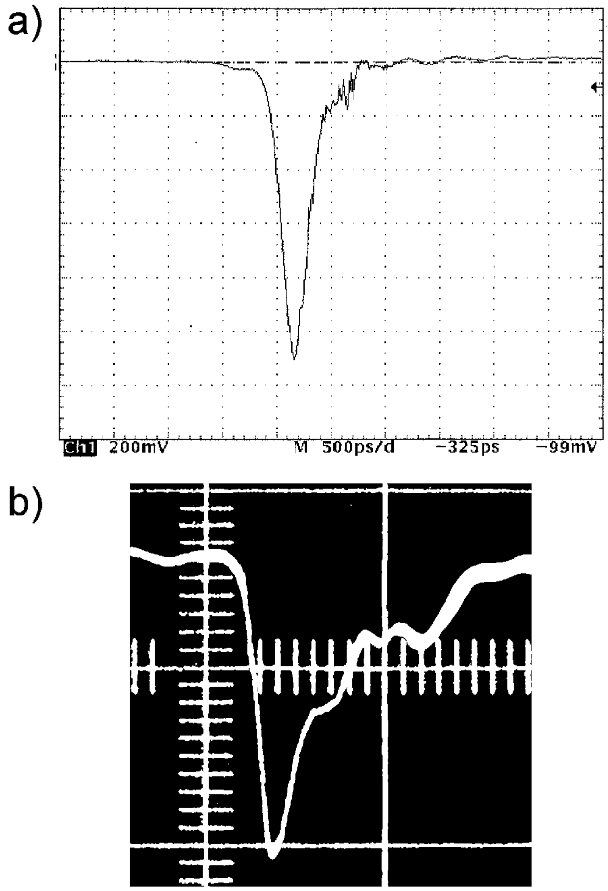

Fig. 23. (a) Envelope of SR pulse having the power of 300 MW, which was recorded by a microwave detector and a stroboscopic oscilloscope at a repetition rate of 1000 Hz. (b) 1.2-GW, 200-ps SR pulse as recorded using a real-time oscilloscope under a single regime.

structure rated at 38 GHz and a pulse magnetic coil with the field of 6.5 T provided conditions when the power conversion was 1.5 ± 0.2 at the output power of the SR pulse up to 1.2 GW and the pulse length of 200 ps [Fig. 23(b)]. Notice that the electron beam power was ~ 650 MW. The radiation power flow density in the SWS was $\sim 1.5\ \mathrm{GW/cm^2}$, which is a record-breaking value for HPM devices today. The energy conversion efficiency in the "beam-electromagnetic wave" system of the microwave source was estimated at 20%–30%.

VI. Conclusion

Summing up the experience gained in development and practical application of small-size pulse generators of the RADAN type, one may draw the following conclusions.

- Shortening of the high-voltage pulse, the electron beam current, and electromagnetic radiation to nanoseconds or smaller not only allows miniaturizing the instruments, but also opens up prospects for fundamentally new research.
- Specific parameters of compact short-pulse high-current instruments may considerably surpass analogous characteristics of installations with long pulses. In particular, extremely high levels of the power and energy flows of electromagnetic radiation are achieved.
- Experiments with small-size pulsed power and accelerating equipment are characterized by rapidness and cost effectiveness in all fields of their application.

References

[1] G. A. Mesyats, *Generation of Powerful Nanosecond Pulses*. Moscow, USSR: Sov. Radio, 1974.
[2] ——, "Pulsed accelerators for relativistic microwave electronics," in *Relativistic High-Frequency Electronics Issue 4* , A. V. Gaponov-Grekhov, Ed. Gorky, USSR: IPF AN SSSR, 1984, pp. 192–216.
[3] A. S. Elchaninov, V. G. Shpak, Y. Y. Urike, and M. I. Yalandin, "RADAN-150 and RADAN-220—A compact pulsed X-ray apparatus," *Defectoscopy*, no. 12, pp. 68–70, Dec. 1984.
[4] A. S. Elchaninov, A. S. Kotov, V. G. Shpak, Y. Y. Urike, and M. I. Yalandin, "RADAN—A compact pulsed repetitive X-ray apparatus and electron accelerators," *Electron. Tech. 4*, no. 2, pp. 33–37, 1987.
[5] G. A. Mesyats, V. G. Shpak, M. I. Yalandin, and S. A. Shunailov, "Compact high-current repetitive pulsed accelerators," in *Proc. 8th IEEE Int. Pulsed Power Conf.*, 1991, pp. 73–77.
[6] ——, "RADAN-EXPERT portable high-current accelerator," in *Proc. 10th IEEE Int. Pulsed Power Conf.*, 1995, pp. 539–543.
[7] S. D. Korovin, "Tesla transformer in a high-current repetitive accelerator," HCEI SB AN SSSR, Tomsk, Tech. Rep. 47, 1988.
[8] G. A. Mesyats, V. G. Shpak, S. A. Shunailov, and M. I. Yalandin, "Desk-top subnanosecond pulser research, development and applications," in *Proc. SPIE Int. Symp.: Intense Microwave Pulses*, vol. 2154, 1994, pp. 262–268.
[9] V. P. Gubanov, S. D. Korovin, and A. S. Stepchenko, "High voltage nanosecond generator with repetition frequency of up to 1 kHz," *Prib. Tekh. Eksp.*, no. 1, pp. 95–98, Jan.–Feb. 1997.
[10] V. G. Shpak, S. A. Shunailov, M. I. Yalandin, and A. N. Dyad'kov, "The RADAN SEF-303A, a small high-current pulsed power supply," *IET*, vol. 36, pp. 106–111, 1993.
[11] M. I. Yalandin and V. G. Shpak, "Compact high-power subnanosecond repetitive-pulse generators," *IET*, vol. 44, no. 3, pp. 285–310, 2001.
[12] B. M. Kovalchuk, G. A. Mesyats, and V. G. Shpak, "Generators of powerful subnanosecond pulses," presented at the IEEE Int. Pulsed Power Conf., Lubbock, TX, 1976, Paper ID5.
[13] V. G. Shpak, M. R. Oulmascoulov, S. A. Shunailov, and M. I. Yalandin, "Amplitude compression of high-voltage pulses in subnanosecond formers on gas spark gaps," in *Dig. Tech. Papers 12th IEEE Int. Pulsed Power Conf.*, vol. 2, 1999, pp. 692–695.
[14] M. I. Yalandin, S. K. Lyubutin, M. R. Oulmascoulov, S. N. Rukin, V. G. Shpak, S. A. Shunailov, and B. G. Slovikovsky, "High peak power and high average power subnanosecond modulator operating at repetition frequency of 3.5 kHz," *IEEE Trans. Plasma Sci.*, vol. 30, pp. 1700–1704, Oct. 2002.
[15] V. G. Shpak, S. A. Shunailov, M. R. Ulmaskulov, M. I. Yalandin, I. V. Pegel, and V. P. Tarakanov, "Compact high-current, subnanosecond electron accelerator," in *Proc. BEAMS'96—11th Int. Conf. High Power Particle Beams*, vol. 2, pp. 913–916.
[16] V. P. Gubanov, S. D. Korovin, I. V. Pegel, V. V. Rostov, A. S. Stepchenko, M. R. Ul'maskulov, V. G. Shpak, S. A. Shunailov, and M. I. Yalandin, "Generation of powerful nanosecond pulses of electromagnetic radiation," *Pis'ma v ZhTF*, vol. 20, no. 14, pp. 89–93, July 1994.
[17] V. G. Shpak, S. A. Shunailov, M. R. Oulmascoulov, and M. I. Yalandin, "Synchronously operated nano- and subnanosecond pulsed power modulators," in *Dig. Tech. Papers of 12th IEEE Int. Pulsed Power Conf.*, vol. 2, 1999, pp. 1472–1475.
[18] S. N. Rukin, S. K. Lyubutin, V. V. Kostirev, and V. A. Telnov, "Repetitive 200 kV nanosecond all-solid-state pulser with semiconductor opening switch," in *Proc. 10th IEEE Pulsed Power Conf.*, vol. 2, 1995, pp. 1211–1214.
[19] F. Y. Zagulov, A. S. Kotov, V. G. Shpak, Y. Y. Urike, and M. I. Yalandin, "RADAN—A compact high-current repetitive electron accelerators," *Prib. Tekh. Eksp.*, no. 2, pp. 146–149, Mar.–Apr. 1989.
[20] V. G. Shpak, S. A. Shunailov, and M. I. Yalandin, "Investigations of compact high-current accelerators RADAN 303 synchronization with nanosecond accuracy," in *Proc. 10th IEEE Int. Pulsed Power Conf.*, 1995, pp. 666–671.

[21] S. D. Korovin, G. A. Mesyats, V. V. Rostov, M. R. Ul'maskulov, K. A. Sharypov, V. G. Shpak, S. A. Shunailov, and M. I. Yalandin, "Subnanosecond source of Ka-band microwave pulses with a 1-GW output peak power," *Pis'ma v ZhTF*, vol. 30, no. 3, pp. 68–74, Feb. 2004.

[22] L. Y. Astanin and A. A. Kostulev, *Bases of the Super Wide-Band Radar Measurements*. Moscow: Radio i Svyaz, 1989.

[23] V. G. Shpak, S. A. Shunailov, M. R. Ulmaskulov, and M. I. Yalandin, "Generation of high-power broadband electromagnetic pulses with PRF of 100 pps," in *Proc. 10th IEEE Int. Pulsed Power Conf.*, 1995, pp. 666–671.

[24] G. A. Mesyats, S. N. Rukin, V. G. Shpak, and M. I. Yalandin, "Generation of high-power subnanosecond pulses," in *Proc. 4th Ultra-Wideband Short-Pulse Electromagnetics Conf.*, 1998, pp. 1–9.

[25] V. G. Shpak, S. A. Shunailov, and M. I. Yalandin, "Matching mode of explosive-emission diode and forming line of pulsed high-voltage nanosecond generator," in *Book of Rec. 7th Symp. High-Current Electronics*, 1988, pp. 87–89.

[26] G. A. Mesyats, V. G. Shpak, M. I. Yalandin, and S. A. Shunailov, "Compact RADAN electron accelerators for testing new radiation technologies and sterilization," *Radiat. Phys. Chem.*, vol. 46, no. 4–6, pp. 489–492, 1995.

[27] V. G. Shpak, M. I. Yalandin, and S. A. Shunailov, "Compact high-current ribbon e-beam diode," in *Proc. 10th Int. Conf. High Power Particle Beams: BEAMS'94*, vol. 1, 1994, pp. 483–486.

[28] S. P. Bugaev, V. P. Il'in, V. I. Koshelev, G. A. Mesyats, V. E. Nechaev, Y. P. Usov, M. I. Fuchs, and B. N. Yablokov, "Formation of intense relativistic electron beams for high power microwave oscillators and amplifiers," in *Relativistic High-Frequency Electronics Issue 1*, A. V. Gaponov-Grekhov, Ed. Gorky, USSR: IPF AN SSSR, 1979, pp. 5–75.

[29] M. I. Yalandin, V. G. Shpak, S. A. Shunailov, and M. R. Ulmaskulov, "Investigation into the formation and transportation of a relativistic high-current electron beam in a permanent-magnet-based focusing system," in *Proc. 17th Int. Symp. Discharges and Electrical Insulation in Vacuum*, vol. 2, 1996, pp. 630–634.

[30] V. P. Gubanov, D. M. Grishin, A. V. Gunin, S. D. Korovin, S. K. Luybutin, G. A. Mesyats, A. V. Nikiforov, V. V. Rostov, S. N. Rukin, B. G. Slovikovsky, K. A. Sharypov, V. G. Shpak, S. A. Shunailov, M. R. Ulmaskulov, and M. I. Yalandin, "High peak power and high average power subnanosecond Ka-Band relativistic BWO," in *Proc. 14th Int. Conf. High-Power Particle Beams: BEAMS 2002*, pp. 263–266.

[31] M. I. Yalandin, V. G. Shpak, S. A. Shunailov, and M. R. Ulmaskulov, "An experimental study of the formation and the dynamics of transportation of a magnetically insulated high-current subnanosecond tubular electron beam," in *Proc. 17th Int. Symp. Discharges and Electrical Insulation in Vacuum*, vol. 2, 1996, pp. 635–639.

[32] V. P. Tarakanov, *User's Manual for Code KARAT*. Springfield, VA: Berkeley Research, 1992.

[33] N. S. Ginzburg, A. S. Sergeev, I. V. Zotova, I. V. Konoplev, A. D. R. Phelps, A. W. Cross, S. J. Cook, P. Aitken, V. G. Shpak, M. I. Yalandin, S. A. Shunailov, and M. R. Ulmaskulov, "Experimental observation of cyclotron superradiance under group synchronism conditions," *Phys. Rev. Lett.*, vol. 78, no. 12, pp. 2365–2368, 1997.

[34] N. F. Kovalev, M. I. Petelin, M. D. Raizer, A. V. Smorgonsky, and L. E. Tsopp, "Generation of powerful pulses of electromagnetic radiation by a flow of relativistic electrons," *Pis'ma v ZhETF*, vol. 18, no. 4, pp. 232–235, Feb. 1973.

[35] A. V. Gunin, A. I. Klimov, S. D. Korovin, I. V. Pegel, S. D. Polevin, and V. V. Rostov, "Relativistic *X*-band BWO with 3-GW output power," *IEEE Trans. Plasma Sci.*, vol. 26, pp. 326–331, June 1998.

[36] V. S. Ivanov, N. F. Kovalev, C. B. Krementsov, and M. D. Raizer, "Relativistic millimeter-band carsinotron," *Pis'ma v ZhTF*, vol. 14, no. 4, pp. 817–820, Feb. 1978.

[37] A. S. Elchaninov, S. D. Korovin, G. A. Mesyats, V. G. Shpak, and M. I. Yalandin, "Generator of powerful nanosecond millimeter-band microwave pulses," in *Techological Applications of High-Current Pulsed Electron Beams*, G. A. Mesyats, Ed. Novosibirsk, USSR: Nauka, 1983, pp. 152–155.

[38] A. S. Elchaninov, S. D. Korovin, G. A. Mesyats, V. V. Rostov, V. G. Shpak, and M. I. Yalandin, "Generation and amplification of microwave radiation with the use of high-current small-size accelerators," in *Proc. 6th Int. Conf. High-Power Particle Beams: BEAMS-86*, 1986, pp. 552–555.

[39] M. I. Yalandin, G. T. Smirnov, V. G. Shpak, and S. A. Shunailov, "High-power repetitive millimeter range back-wave oscillators with nanosecond relativistic electron beam," in *Proc. 9th IEEE Int. Pulsed Power Conf.*, vol. 1, 1993, pp. 388–391.

[40] A. S. Elchaninov, F. Y. Zagulov, S. D. Korovin, G. A. Mesyats, and V. V. Rostov, "Microwave pulse shortening in the relativistic carsinotron," *Pis'ma v ZhTF*, vol. 6, no. 19, pp. 1168–1171, Oct. 1981.

[41] M. I. Yalandin, V. G. Shpak, and V. P. Tarakanov, "Experimental observation of modulation modes of powerful microwave pulses produced by a 5-Nanosecond width Ka-Band backward wave oscillator," in *Dig. Tech. Papers IEEE Int. Pulsed Power-Plasma Science Conf.*, 2001, pp. 544–547.

[42] R. H. Dicke, "Coherence in spontaneous radiation processes," *Phys. Rev.*, vol. 93, pp. 99–110, 1954.

[43] N. S. Ginzburg, Y. V. Novozhilova, and A. S. Sergeev, "Superradiance of ensembles of classical electron-oscillators as method for generation of ultrashort electromagnetic pulses," *Nucl. Instrm. Methods Phys. Res. A, Accel. Spectrom. Detect. Assoc. Equip.*, vol. 341, pp. 230–233, 1994.

[44] N. S. Ginzburg, I. V. Zotova, Y. V. Novozhilova, A. S. Sergeev, M. R. Ul'maskulov, V. G. Shpak, S. A. Shunalov, M. I. Yalandin, A. D. R. Phelps, A. W. Cross, and S. Cook, "Generation of ultrashort pulse based on the superradiance of isolated electron bunches," *Izv. Vuzov: Appl. Nonlinear Dyn.*, vol. 6, no. 1, pp. 38–53, Jan. 1998.

[45] M. I. Yalandin, S. A. Shunalov, V. G. Shpak, N. S. Ginzburg, I. V. Zotova, A. S. Sergeev, A. D. R. Phelps, A. W. Cross, and P. Aitken, "Cherenkov superradiance from a subnanosecond electron bunch in a sectional decelerating system," *Tech. Phys. Lett.*, vol. 23, no. 12, pp. 948–950, Dec. 1997.

[46] N. S. Ginzburg, S. P. Kuznetsov, and T. N. Fedoseeva, "Theory of transit processes in the relativistic BWO," *Izv. Vusov, Radiophys.*, vol. 21, no. 7, pp. 1037–1052, 1978.

[47] M. I. Yalandin, V. G. Shpak, S. A. Shunailov, M. R. Oulmaskoulov, N. S. Ginzburg, I. V. Zotova, Y. V. Novozhilova, A. S. Sergeev, A. D. R. Phelps, A. W. Cross, S. M. Wiggins, and K. Ronald, "Generation of powerful subnanosecond microwave pulses in the range of 38–150 GHz," *IEEE Trans. Plasma Sci.*, vol. 28, pp. 1615–1619, Oct. 2000.

[48] N. S. Ginzburg, Y. V. Novozhilova, I. V. Zotova, A. S. Sergeev, N. Y. Peskov, A. D. R. Phelps, S. M. Wiggins, A. W. Cross, K. Ronald, W. He, V. G. Shpak, M. I. Yalandin, S. A. Shunailov, M. R. Ulmaskulov, and V. P. Tarakanov, "Generation of powerful subnanosecond microwave pulses by intense electron bunches moving in a periodic backward wave structure in the superradiative regime," *Phys. Rev. E*, vol. 60, pp. 3297–3304, 1999.

[49] A. A. Eltchaninov, S. D. Korovin, V. V. Rostov, I. V. Pegel, G. A. Mesyats, S. N. Rukin, V. G. Shpak, M. I. Yalandin, and N. S. Ginzburg, "Production of short microwave pulses with a peak power exceeding the driving electron beam power," *Laser Part. Beams*, vol. 21, pp. 187–196, 2003.

[50] S. D. Korovin, I. K. Kurkan, V. V. Rostov, and E. M. Totmeninov, "Relativistic BWO with a lumped resonant reflector," *Izv. Vusov: Radiophys.*, vol. 42, no. 12, pp. 1189–1196, 1999.

[51] A. I. Klimov, S. D. Korovin, V. V. Rostov, M. R. Ulmaskulov, V. G. Shpak, S. A. Shunailov, and M. I. Yalandin, "Highly efficient generation of subnanosecond microwave pulses in Ka-Band relativistic BWO," *IEEE Trans. Plasma Sci.*, vol. 30, pp. 1120–1125, June 2002.

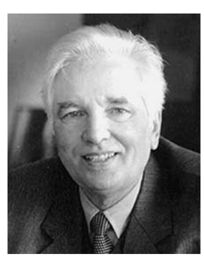

Gennady A. Mesyats was born in 1936. He received the M.Sc. Candidate Sci., and Dr.Sci. degrees from Tomsk Polytechnic Institute in 1958, 1961, and 1964, respectively.

To perform scientific research in pulsed power, he established the Institute of High Current Electronics (Tomsk, Russia, 1977) and the Institute of Electrophysics (Sverdlovsk, Russia, 1986), having been Director of the latter since 1986. He has authored and coauthored over 500 scientific articles and 15 monographs. His scientific interests include electrical discharges in gas and vacuum, pulsed power, gas lasers, etc.

Prof. Mesyats is the Vice President of the Russian Academy of Sciences. He is a member of many international and Russian scientific institutions, such as the American Physical Society, the American Optical Society, and the SPIE. He has been awarded numerous national and international awards in science, including the first Global Energy Award in 2003.

Sergei D. Korovin received the M.Sc. degree in plasma physics from Novosibirsk State University in 1975 and the Candidate Sci. and Dr.Sci. degrees from the Institute of High Current Electronics, Russian Academy of Science, Tomsk, in 1981 and 1991, respectively.

Since 1975, he has been with the Institute of High Current Electronics, Tomsk, Russia and is currently Director of the Institute and Head of the Physical Electronics Department. He has authored or coauthored about 200 journal and conference papers. His research interests include microwave physics, relativistic high-current electronics, and physics of high-current electron accelerators.

Dr. Korovin was elected Member of Russian Academy of Sciences in 2003. He was awarded the Komsomol Award in science in 1979 and the State Award of Russian Federation in science in 1998.

Vladislav V. Rostov received the M.Sc. degree in plasma physics from Novosibirsk State University in 1978 and the Candidate Sci. and Dr.Sci. degrees from the Institute of High Current Electronics, Russian Academy of Science, Tomsk, in 1985 and 2001, respectively.

He has been with the Institute of High Current Electronics since 1978. He is now Leader of a research group dealing with theoretical investigations in high-power microwave electronics.

Dr. Rostov was awarded the Komsomol Award in science in 1987.

Valery G. Shpak was born in 1944. He received the M.Sc. and Candidate Sci. degrees in electrovacuum devices from the Radioelectronics Institute, Tomsk, in 1967 and 1980, respectively, and the Dr.Sci. degree in 1989 from the Institute of High Current Electronics, Tomsk.

He was formerly with the Institute of High Current Electronics, Tomsk, and since 1986, he has been Head of the Laboratory of Electron Accelerators at the Institute of Electrophysics, Ekaterinburg, Russia. He is also a Deputy Director of the Institute of Electrophysics. Most of his publications are devoted to the investigation of high-speed processes and the research and design of compact pulsed power equipment for the nano- and subnanosecond range.

Dr. Shpak has been a Corresponding Member of the Russian Academy of Sciences since 1997. He was awarded the State Award of Russian Federation in science in 1998.

Michael I. Yalandin was born in 1956. He received the M.Sc. degree in plasma physics from Novosibirsk State University in 1979 and the Candidate Sci. and Dr.Sci. degrees from the Institute of High Current Electronics, Tomsk, in 1986 and 1996.

He is currently with the Institute of Electrophysics, Ekaterinburg, Russia, where he is Head of the group currently engaged in the investigation and development of compact high-voltage nanosecond and subnanosecond modulators, pulsed electron accelerators, and high-power sources of coherent and broadband microwaves.

Dr. Yalandin was elected Corresponding Member of the Russian Academy of Sciences in 2003. He was awarded the Komsomol Award in science in 1987 and the State Award of Russian Federation in science in 1998.